JACS
JOURNAL OF THE AMERICAN CHEMICAL SOCIETY

ARTICLE

pubs.acs.org/JACS

DNA-Based Optomechanical Molecular Motor

Martin McCullagh, Ignacio Franco, Mark A. Ratner, and George C. Schatz*

Department of Chemistry, Northwestern University, Evanston, Illinois 60208-3113, United States

Supporting Information

ABSTRACT: An azobenzene-capped DNA hairpin coupled to an AFM is presented as an optically triggered single-molecule motor. The photoinduced trans to cis isomerization of azobenzene affects both the overall length of the molecule and the ability of the DNA bases to hybridize. Using a combination of molecular dynamics simulations and free energy calculations the unfolding of both isomers along the O5′−O3′ extension coordinate is monitored. The potentials of mean force (PMFs) along this coordinate indicate that there are two major differences induced by photoisomerization. The first is that the interbase hydrogen bond and stacking interactions are stable for a greater range of extensions in the trans system than in the cis system. The second difference is due to a decreased chain length of the cis isomer with respect to the trans isomer. These differences are exploited to extract work in optomechanical cycles. The disruption of the hairpin structure gives a maximum of 3.4 kcal mol^{-1} of extractable work per cycle with an estimated maximum efficiency of 2.4%. Structure−function insights into the operation of this motor are provided, and the effect of the cantilever stiffness on the extractable work is characterized.

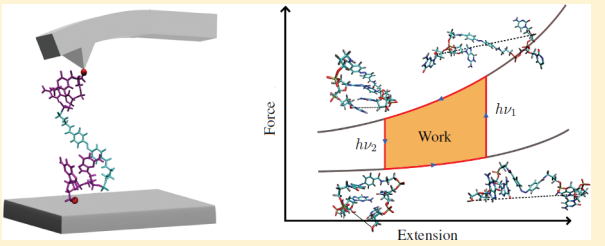

INTRODUCTION

Recent technological advances have provided the tools to manipulate and measure the properties of single molecules.[1−3] Single-molecule pulling, in particular, permits inducing molecular unfolding/refolding events while simultaneously performing thermodynamic measurements.[4−6] Specifically, these experiments provide information about the force exerted during the extension from which the molecular Helmholtz free energy profile along the extension coordinate can be extracted.[7−10]

The basic setup of a single-molecule pulling experiment is schematically shown in Figure 1. In it, one end of a molecule is attached to a surface while the other end is attached to an atomic force microscope (AFM) tip coupled to a cantilever. In these experiments, the distance between the surface and the cantilever (L) is controlled while the force exerted fluctuates. The force is determined by measuring the deflection of the harmonic cantilever from its equilibrium position $F(t) = -k(\xi(t) - L)$, where $\xi(t)$ is the fluctuating molecular end-to-end distance and k is the cantilever stiffness.

A particularly rich and promising use of this force spectroscopy setup is for constructing molecular motors. The basic idea behind these motors is to supplement the force spectroscopy with an external stimulus capable of reversibly changing the elastic properties of the molecule that is being pulled. With these two elements a single-molecule analog of a thermodynamic cycle is set up in which the molecule effectively acts as an energy transducer, converting the externally supplied energy into mechanical work. A schematic of such a cycle in the force−extension plane is shown in Figure 2. The molecule in its "soft" version is first extended by varying the distance between the surface and the cantilever from L_1 to L_2. At this extension, the external stimulus is applied to change the elastic properties of the molecule. The stiffened molecule is contracted by modifying L from L_2 to L_1. The cycle is closed by applying a second stimulus that returns the molecule to its original state. The net extractable work is given by the shaded area enclosed by the force−extension isotherms during the cycle.

The advantage of this setup with respect to most other reported examples of molecular motors[11] is that the AFM acts as an interface with the outside world that permits extracting any generated work. Importantly, the setup provides means to *quantitatively* compare the ability of different chemical motifs to transduce externally supplied energy into mechanical work through measurements of the force during extension.

Two experimental realizations of this concept have been reported to date. In the prototype of Hugel et al.,[12,13] the molecule is a poly(azopeptide) and the external stimulus is light. The radiation is used to induce cis/trans isomerization of the azobenzene moieties.[14−17] The cis version of the polymer is stiffer because the end-to-end distance of the constituent monomers is 0.6 Å shorter than their trans counterparts.[18] A second prototype developed by Shi et al.[19] employs a redox process in order to tune the elastic properties of a polyferrocenylsilane by changing the charge density along the polymer.

In this paper we propose a novel molecular motor of this class that takes advantage of the cis/trans photoinduced isomerization of azobenzene to modify the elastic properties of a DNA hairpin. The prototype consists of two guanine (G)-cytosine (C) base pairs capped by an azobenzene linker, see Figure 1. The isomerization of the azobenzene is used to disrupt the stacking and hydrogen bond network in the hairpin structure, thus changing the elasticity of the molecule. These disruptions amplify the effect

Received: October 8, 2010
Published: February 22, 2011

dx.doi.org/10.1021/ja109071a | J. Am. Chem. Soc. 2011, 133, 3452–3459

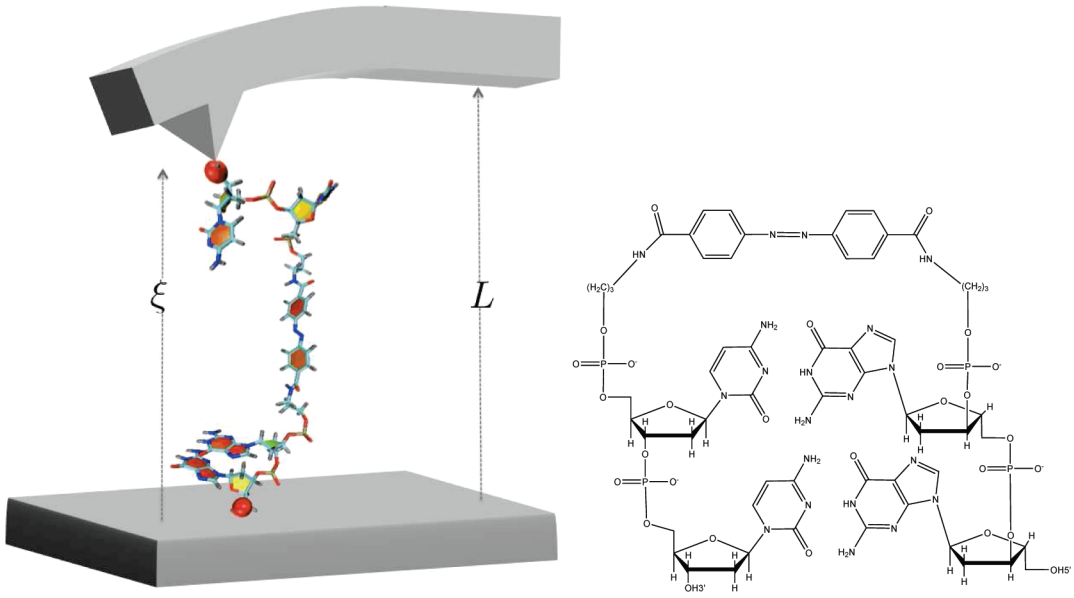

Figure 1. Schematic of a single-molecule pulling setup and of the DNA-based molecular motor. The molecule is attached by its ends to a surface at the terminal O5′ atom and an AFM tip at the terminal O3′ atom. The distance between the surface and the cantilever (L) is controlled, while the deflection of the cantilever from its equilibrium position measures the instantaneous applied force on the molecule by the cantilever $F = -k(\xi - L)$. Here ξ is the fluctuating molecular end-to-end distance and k the cantilever stiffness. The structure of the photoresponsive DNA that provides the basis for the motor is shown in the right panel. It consists of two guanine-cytosine base pairs connected by an azobenzene linker. Light is used to induce cis−trans isomerization in the azobenzene, thus modifying the molecular elasticity properties.

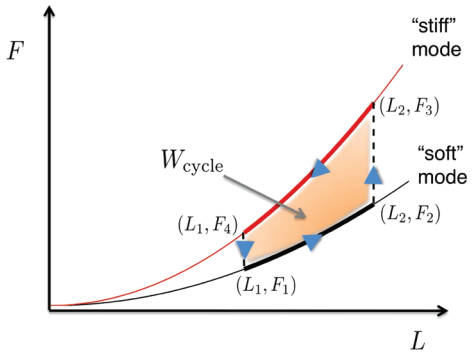

Figure 2. Single-molecule cycle used for work extraction in a force spectroscopy setup. The molecule in its soft mode is extended by varying the distance between the surface and the cantilever from L_1 to L_2. At this extension an external stimulus is applied capable of making the molecule stiffer. The molecule in its stiff version is then contracted by varying L from L_2 to L_1. The cycle is closed by applying a second stimulus that reverses the induced changes on molecular elasticity. The next extractable work W_{cycle} is given by the shaded area in the figure.

of the cis/trans isomerization, leading to a mechanism for energy transduction that is fundamentally different from the one previously observed in poly(azopeptide)s.

The use of light to power molecular motors[20−23] and molecular level force probes[24] has a distinguished tradition due to its versatility and the ultrafast picosecond reaction timescale that is usually involved in photoexcitation. The photoisomerization of azobenzene, specifically, has been shown to be robust even in hindering environments,[25,26] making it a particularly useful component in motor design. In DNA, azobenzene has been intercalated between bases to photoinduce melting in double-stranded structures.[27−30] Analogous molecules to the one proposed here with stilbene caps instead of azobenzene have been synthesized before,[31] but their potential as energy transducers has not been quantified.

The maximum extractable work in the cycle shown in Figure 2 is achieved when the pulling and contracting are performed quasistatically. In the canonical ensemble, the reversible work per cycle is given by

$$W_{cycle} = \frac{1}{\beta} \ln \frac{Z_2(L_1) Z_1(L_2)}{Z_2(L_2) Z_1(L_1)} \qquad (1)$$

where $\beta = 1/k_B T$ is the inverse temperature and $Z_i(L)$ is the partition function of the molecule plus the cantilever at extension L. Subindex i = 1,2 denotes the two possible (cis and trans) molecular modes. Equation 1 takes into account that the properties measured in single-molecule pulling experiments are those of the molecule plus the cantilever. The partition function of the composite molecule plus cantilever system admits a simple expression[10]

$$Z_i(L) = \int \mathrm{d}\xi \, \exp\{-\beta[\phi_i(\xi) + V_L(\xi)]\} \qquad (2)$$

where $\phi_i(\xi)$ is the molecular potential of mean force PMF (the Helmholtz free energy profile) along the end-to-end coordinate ξ for the molecule in mode i and $V_L(\xi) = k(\xi - L)^2/2$ is the potential due to a cantilever of stiffness k at extension L. The convention that net extractable work is positive is adopted throughout the paper.

The molecular elastic properties are completely characterized by $\phi_i(\xi)$. Here, this quantity is estimated using atomistic molecular dynamics (MD) and the weighted histogram analysis method (WHAM).[32,33] In addition to determining the ability of azobenzene-capped DNA dimers to transform electromagnetic radiation into mechanical work, the simulations presented below provide a detailed account of the rather intricate unfolding

dx.doi.org/10.1021/ja109071a |J. Am. Chem. Soc. 2011, 133, 3452–3459

dynamics of DNA when disrupted by the photoswitchable cap. This complements previous studies on pristine RNA[34−36] and DNA[37] unfolding. The resulting structure−function insights are important for future DNA motor design.

This manuscript is organized as follows. The specifics of the MD simulations and the free energy computations are given in the Methods section. The Results and Discussion section is divided into three parts. The first part discusses the potential of mean force and the unfolding pathways of the cis and trans structures. The second part introduces the possible modes of operation for net work extraction and the efficiency of the device. The last part discusses the photoinduced structural changes on DNA that are responsible for the extractable work. The main findings are summarized in the Conclusions section.

METHODS

The DNA bases were built using the NAB module in Amber 10[38] and simulated using the CHARMM27 force field.[39,40] The azobenzene unit was built separately with standard CHARMM27 atom types being chosen for all atoms except the central nitrogens. Bond and angle force field parameters for these nitrogens were taken to be equivalent to the nucleic acid aromatic carbon (CNA). Most dihedral angle parameters were taken as equivalent to the CNA values with the exception of C−N−N−C and C−C−N−N. These two dihedral angles are significantly different in the cis and trans forms. The equilibrium values for these were fitted to B3LYP/6-31+G** calculations. The C−N−N−C equilibrium values were taken to be 180° for trans and 0° for cis with a force constant of 14.0 kcal mol $^{-1}$. The C−C−N−N equilibrium values were taken to be 0° and 180° for trans and −50° and 130° for cis with a force constant of 4.425 kcal mol^{-1}. The Lennard−Jones nonbonding parameters for the central nitrogens were taken to be the same as the other CHARMM27 nitrogens. Charges for all azobenzene atoms were assigned by the standard procedure of fitting the HF/6-31G*-determined electrostatic potential to atomic charges using the restrained electrostatic potential (RESP) module in Amber.[41] The resulting set of charges is included in the Supporting Information. The final structure for azobenzene in both forms compares qualitatively well with crystallographic data.[42,43]

For the purpose of determining the maximum extractable work, it is necessary to quantify the elastic properties of the system in the cis and trans forms. For this, we assume that the molecule in either form is in a state of local equilibrium. Direct modeling of the isomerization event is not required for the present purposes (see ref 44 for a general description of isomerization through conical intersections). We suppose that pulling and contracting of our system occurs under reversible conditions. The pulling direction is taken to be along the axis defined by the O5′−O3′ molecular end-to-end coordinate ξ. During pulling, the O5′ atom was restrained by a stiff isotropic harmonic potential that mimicked the molecular attachment to the surface. Simultaneously, the opposite O3′ atom was subject to a harmonic bias that mimics the effect of the AFM cantilever on the molecule. The cantilever is taken to have a stiffness of k_0 = 1.1 N/m (1.58273 kcal mol^{-1} Å^{-2}) along the pulling coordinate ξ and to be stiff in the perpendicular directions. This stiffness was preferred over softer cantilevers because it simplifies sampling.[45] The sampling along the extension coordinate required to reconstruct the potential of mean force proceeded as follows: The distance, L, between the surface and the cantilever was fixed at several different values along the extension coordinate. After an initial energy minimization in vacuum the system was placed in a pre-equilibrated solvent box. The energy of the solvated system was minimized and the system allowed to equilibrate for 4 ns. Subsequently, the dynamics was followed for 8 ns and the end-to-end distance ξ recorded every 1 ps. In total, 121 extensions for the cis form and 155 extensions for the trans form were simulated. Values of L ranged from 6.75 to 44.75 Å, while ξ ranged from 2.9 to 44.9 Å. Total analyzed simulation time was 0.97 μs for the cis system and 1.24 μs for the trans system.

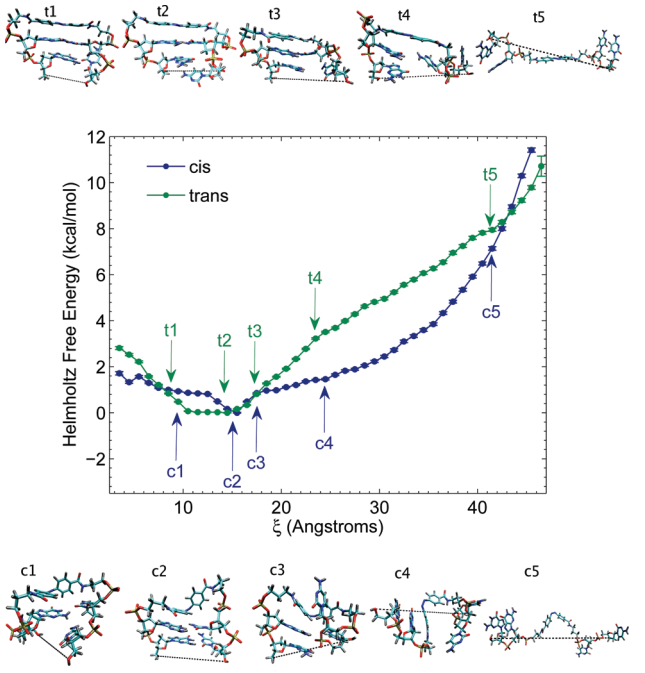

Figure 3. Potential of mean force along the end-to-end distance coordinate for the azobenzene-capped DNA hairpin. Snapshots of structures adopted during the unfolding are shown in the top panel (**t1**−**t5**) for the trans conformation and the bottom panel (**c1**−**c5**) for the cis conformation. The error bars correspond to twice the standard deviation obtained from a bootstrapping analysis. Note the considerable changes induced by photoisomerization on the free energy profile.

All molecular dynamics simulations were performed using NAMD[46] at 300 K in the NVT ensemble with a Langevin thermostat with a damping coefficient of 5.0 ps^{-1}. The total system is composed of 178 DNA hairpin atoms, 4 sodium ions, and 1731 TIP3P water molecules in a 27.1 Å × 34.7 Å × 56.3 Å box. An integration time step of 2 fs was used in combination with the SHAKE algorithm. A real space cutoff of 12 Å with a switch distance of 10 Å and the particle mesh Ewald method are used to compute nonbonded interactions.

The molecular potential of mean force $\phi(\xi)$ along the end-to-end distance coordinate was reconstructed from the biased simulations at extensions L using the weighted histogram analysis method (WHAM),[32,33] as described in detail elsewhere.[10] The PMF is an intrinsic molecular property that is independent of the cantilever stiffness. In the WHAM procedure we employed bins of 1 Å along ξ and used as a convergence criteria an average difference of 10^{-7} kcal mol^{-1} among consecutive estimates of the free energy in the self-consistent procedure. The resulting free energy profiles are subsequently used to estimate the extractable work using eqs 1 and 2. The PMF also permits estimating the force−extension isotherms for the composite molecule plus cantilever system for any value of the force constant k. Specifically, the average force exerted on the system at extension L is given by

$$\langle F\rangle_L = -\frac{1}{\beta}\frac{\partial \ln[Z(L)/Z_0]}{\partial L} \qquad (3)$$

where Z_0 is an arbitrary constant used to make the argument in the logarithm dimensionless.

RESULTS AND DISCUSSION

Potential of Mean Force and Unfolding Pathway. The PMFs for both the cis and the trans conformations of the

dx.doi.org/10.1021/ja109071a |J. Am. Chem. Soc. 2011, 133, 3452–3459

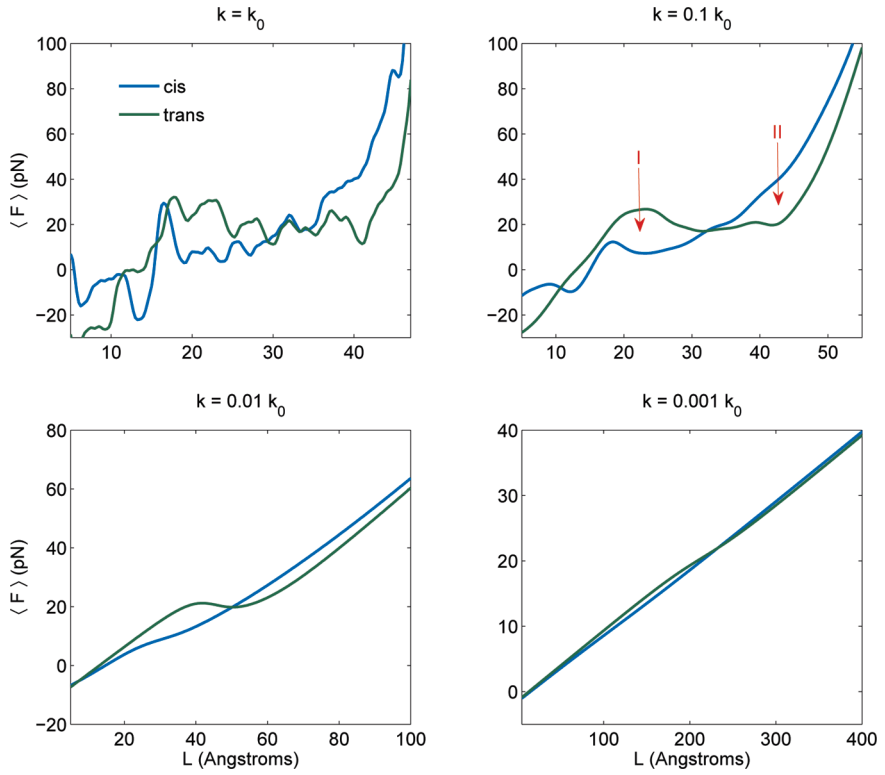

Figure 4. Force−extension isotherms during the pulling. The panels show the elastic behavior of both the cis and the trans structures when pulled using cantilevers of different stiffness k (k_0 = 1.1 N/m). Note that the cis structure is softer than the trans one for short extensions and stiffer for long extensions. This inversion in the relative stiffness between the two molecular modes leads to two possible ways of work extraction, labeled I and II in the upper right panel.

azobenzene-capped DNA hairpin are shown in Figure 3. Snapshots of relevant structures adopted during the unfolding process are given in the top panel for trans (**t1**−**t5**) and the bottom panel for cis (**c1**−**c5**). Generally speaking, regions of convexity along the PMF correspond to mechanically stable molecular conformations, while regions of concavity signal molecular unfolding events.[10] These concave regions lead to mechanical instabilities where the force decreases with the extension $(\partial\langle F\rangle_L/\partial L) < 0$ during the pulling.

The PMF of the trans conformation shows a convex region for ξ < 17 Å representing the folded state, a mostly concave region for 17 Å < ξ < 40 Å where the molecule unfolds, followed by another region of convexity that corresponds to the unfolded state. The unfolding region exhibits some convex intervals signaling marginally stable intermediates encountered during the unfolding. The folded native phase is for 11 Å < ξ < 15 Å. For ξ < 11 Å the structure is contracted, and this leads to a disruption of the terminal base, **t1** being a representation in which the terminal cytosine flips out. For $\xi \approx$ 11 Å structures with a stacked terminal base pair (e.g., **t2**) become stable. These conformations are comparable in energy to the hydrogen-bonded terminal base pair due to possible backbone frustration caused by the trans azobenzene cap as well as normal DNA end fraying.[47,48] The unfolding of the trans structure begins at ξ = 17 Å and is generally initiated by the flipping out of the terminal cytosine (cf. **t3**). This event is followed by the breaking of the hydrogen bonds in the inner base pair at $\xi \approx$ 24 Å, as is represented by snapshot **t4** . Subsequent pulling induces the breaking of stacking interactions between the azobenzene unit and the neighboring bases. By ξ = 40 Å the hairpin is completely unfolded.

The native state of the cis conformation occurs in the 13 Å < ξ < 17 Å region of the extension coordinate in which both GC base pairs form Watson−Crick structures as depicted in **c2** . This conformation, however, is barely stable with a well depth of less than 1 kcal mol^{-1} with respect to unstacked structures, leading to coexistence between the two at room temperature. There are two narrow concave regions along the PMF that signal conformational transitions. The resulting mechanically stable contracted region (ξ < 12 Å) is characterized by a disorganized globular structure, such as **c1**, with very little hydrogen bonding and stacking. In turn, the resulting unfolded region ξ > 18 Å exhibits only stacking interactions. The hydrogen bonding of both base pairs is broken in a narrow region around $\xi \approx$ 17 Å.

Elastic Properties, Extractable Work, and Efficiency. The photoinduced changes in the PMFs of the hairpin structure provide the basis for an optomechanical motor. To see this, consider first the force−extension isotherms shown in Figure 4 for the cis and trans structures when pulled with cantilevers of different stiffness. Here we focus on the k = 0.1 k_0 = 0.11 N/m case since this force constant falls in an experimentally preferred range. In the trans case the force initially increases, observes a drop between L = 22 and 42 Å, and then increases again. The drop in the force is due to molecular unfolding during pulling. The computed stress maximum compares well with experimentally determined values for analogous systems.[49] In the cis mode the unfolding event occurs at shorter $L \approx$ 18 Å because the DNA hairpin is less mechanically stable. Note that for short extensions the trans structure is stiffer than the cis one because of the disruption of the hydrogen bonding and stacking interaction upon trans-to-cis photoisomerization. At long extensions,

dx.doi.org/10.1021/ja109071a |J. Am. Chem. Soc. 2011, 133, 3452–3459

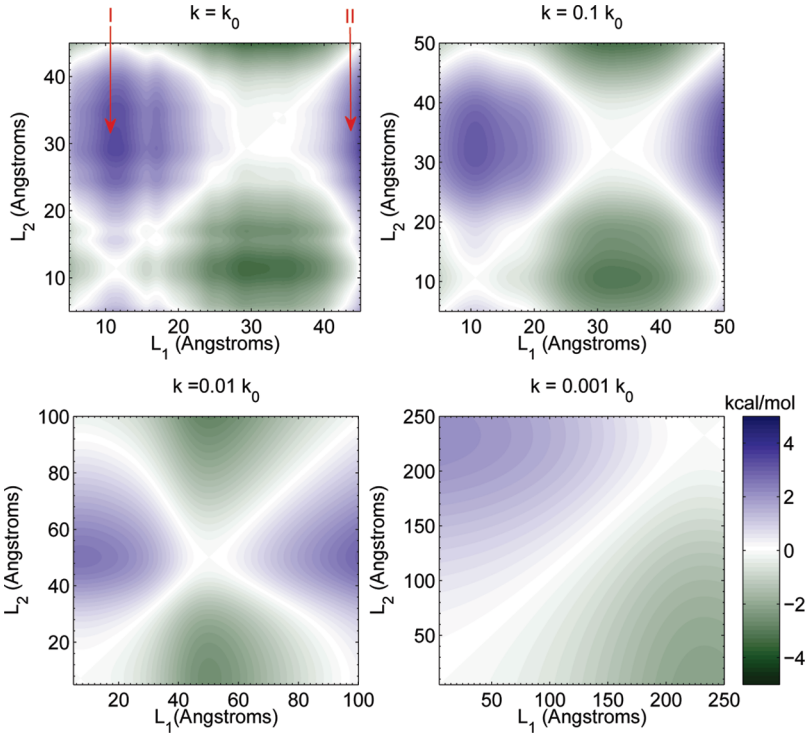

Figure 5. Net extractable work W_{cycle} from the DNA-based motor. The meaning of the extensions L_1 and L_2 is specified in Figure 2. The color code is given in the lower right. Note the two possible modes of work extraction (I and II) and the substantial effect that the cantilever stiffness has on the extractable work.

however, this effect is reversed with the cis form becoming stiffer due to its shorter length.

For work extraction, we consider optomechanical cycles in which the molecule in the cis form is elongated (or contracted) by varying L from L_1 to L_2. At L_2, 420 nm light is applied to induce a cis-to-trans isomerization. Subsequently, L is varied from L_2 back to L_1 and 365 nm light is applied to turn the trans mode into the cis mode and close the cycle. Figure 5 shows the net extractable work for different L_1 and L_2 values and different cantilever stiffnesses.

The basic features of the $F-L$ isotherms lead to two distinct modes of work extraction, labeled I and II in Figures 4 and 5, that operate in opposite ways. Mode I is characteristic of DNA since it is based on the disruption of the paired bases. Mode II, in turn, is equivalent to the mechanism for energy transduction used in poly-azopeptides[12,13] in which the change of length of the molecule upon photoisomerization is the origin of the optomechanical effect. While in mode I the trans form is the "stiff" version of the molecule, in mode II the cis form plays that role. These two possible modes of work extraction can be isolated by properly choosing the L_1 and L_2 parameters for motor operation.

Since the properties measured during the pulling are those of the molecule plus cantilever, the extractable work depends strongly on the cantilever stiffness used. We observe, in Figure 4, that the maximum extractable work is obtained when stiff cantilevers are employed since none of the optomechanical effect is wasted on deflecting the cantilever. Note that for soft cantilevers the extractable work becomes negligible. This is because the native end-to-end distances of the DNA hairpin in its cis and trans modes are approximately equal and because in the soft-spring limit the slope of the force−extension isotherm is independent of the molecule and given by $\partial\langle F\rangle_L/\partial L \approx k + O(k^2)$.[10]

For Mode I, the maximum extractable work is 3.4 kcal mol^{-1} per cycle obtained by using $k = k_0$, L_1 = 11 Å, and L_2 = 30 Å. These two extensions naturally coincide with curve crossings of the associated $F-L$ isotherms in Figure 4. For Mode II, the maximum extractable work in the parameter space explored is 3.5 kcal mol^{-1} per cycle obtained using $k = k_0$, L_1 = 44 Å, and L_2 = 30 Å. Note that in this case the order of L_1 and L_2 for net work extraction is reversed with respect to Mode I. Since Mode II operates in a regime where chemical bonds are stretched, the estimated extractable work is not expected to be quantitative since the CHARMM force field is not parametrized to accurately describe this. This is in stark contrast to Mode I that operates in a regime for which the CHARMM force field is well parametrized.

A simple estimate of the efficiency of this motor can be obtained as follows. The net work extracted per cycle in Mode I is 2.4×10^{-20} J. The quantum yield of the trans to cis isomerization using 365 nm (5.5×10^{-19} J) photons is ~0.1, and hence, 10 of these photons are required per cycle.[16] In turn, the quantum yield of the cis to trans isomerization using 420 nm (4.7×10^{-19} J) photons is ~0.5.[16] The total optical energy required per cycle is then ~6.5×10^{-18} J for a net operation efficiency of ~0.4%. An analogous calculation for the poly(azopeptide) prototype yielded an efficiency of ~0.08%.[13] This indicates that the stacking and hydrogen bonding of the hairpin structure amplifies the photoinduced changes of azobenzene, leading to a mode for work extraction that is fundamentally different and a factor of 5 more efficient than the one observed for poly(azopeptide)s. The maximum possible efficiency of this motor is obtained by supposing that every photon is absorbed and induces photoisomerization to yield ~2.4%. While the major energy waste is expected to arise due to the inherent inefficiencies of azobenzene's photoisomerization processes, other factors may

dx.doi.org/10.1021/ja109071a | J. Am. Chem. Soc. 2011, 133, 3452–3459

impact the motor efficiency. These include spectral overlap of the photoisomerization processes, dependency of photoisomerization quantum yield on applied force, sample heating, and other complex dissipative effects.

Structure−Function Relations in Motor Operation. The structural origins of the work extraction are important guides to understanding our current molecular motor and to aiding in the design of a better one. In order to determine the important structural features, order parameters as a function of end-to-end distance were monitored. A number of order parameters were considered with the most elucidating set being the base−base interaction energies, similar to the study of Hagan et al.[50] The important pairwise interaction energies between the bases are plotted in Figure 6. For clarity, in the upcoming discussion we label the bases GUA1, GUA2, AZO, CYT4, and CYT5 in the manner specified in the figure. Interactions between the bases were computed as the sum of the Lennard−Jones and Coulomb interactions between all atoms of one base with all atoms of the other. Figure 6A contains hydrogen-bonded type pairs (GUA1-CYT5 and GUA2-CYT4), Figure 6B contains azobenzene and adjacent base stacking pairs (AZO-CYT4 and AZO-GAU2), while Figure 6C contains cross terms (GUA1-CYT4 and GUA2-CYT5). Bold lines correspond to the trans conformation and the thin lines to the cis one.

The maximum work extraction for Mode I uses $k = k_0$, $L_1 = 11$ Å, and $L_2 = 30$ Å (recall Figure 5). For this cantilever stiffness the extension L is approximately equal to the end-to-end distance ξ. The difference between the cis and the trans curves at $\xi = 11$ and 30 Å are thus the most important aspects of Figure 6 for work extraction. The cis/trans differences at $\xi = 30$ Å are negligible for all interactions; thus, we focus on $\xi = 11$ Å. For the hydrogen bond type interactions in Figure 6A, the major difference between cis and trans is the stability of the inner base pair (GUA2-CYT4) at $\xi = 11$ Å. The cis structure has a very narrow region around $\xi = 15$ Å in which the inner base pair is fully formed, whereas the trans structure has a fully formed inner base pair for $\xi < 17$ Å. The added stability of the trans inner base pair at $\xi = 11$ Å causes the trans structure to be stiffer in this region.

For the stacking interactions plotted in Figure 6B, the major difference between the cis and trans structures at $\xi = 11$ Å is the AZO-CYT4 interaction. Again, the trans structure has a stable interaction at these short distances, while the cis structure shows little stacking stability. The cis/trans difference in the AZO-GUA2 interactions is fairly small, suggesting that the cis isomer of azobenzene can also remain stacked to one neighboring base and does so with the guanine. In turn, the cross-term interaction energies plotted in Figure 6C show that typical stacking and hydrogen bond interactions do not tell the whole story. There is a dramatic difference between the cis and the trans interaction energy of the terminal guanine to inner cytosine (GUA1-CYT4). At $\xi = 11$ Å, this interaction energy reaches a minimum of ~ -12 kcal mol^{-1} for the trans structure, while it is almost negligible for the cis structure. This is evidence of a fairly ordered contracted structure for the trans isomer and a disordered one for the cis isomer.

Work extraction from this motor arises due to a rather intricate interplay of induced conformational changes onset by the cis/trans isomerization. The three major interaction energies which contribute to the extractable work for our motor are inner base pair hydrogen bonding, azobenzene-cytosine stacking, and terminal guanine-inner cytosine interaction. Surprisingly, perhaps, the hydrogen bonding of the terminal base as well as the normal DNA base−base stacking are not substantially affected by the isomerization and play little role in the motor operation.

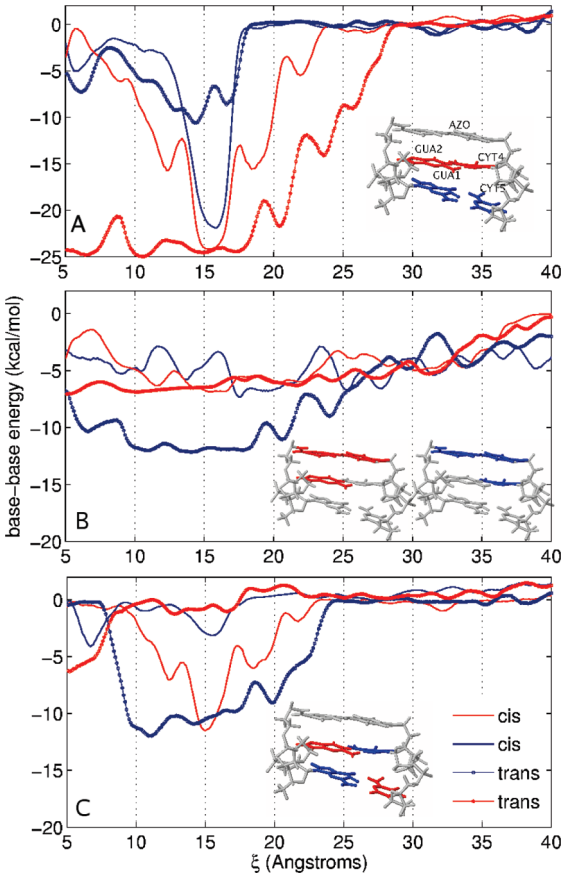

Figure 6. Base−base interactions during unfolding of the DNA hairpin. The interaction energies plotted in each panel are specified by the color-coded structures. Thick (or thin) lines correspond to the trans (or cis) conformation. The top panel shows interactions that are mostly hydrogen bonding in nature, the middle panel shows stacking, while those shown in the bottom panel are mixed. The bases are labeled GUA1, GUA2, AZO, CYT4, and CYT5 starting with the terminal 5′ base as shown in the top panel.

CONCLUSIONS

We proposed a prototype of a molecular motor attached to an AFM that is based on photoisomerization of a DNA hairpin consisting of two guanine-cytosine base pairs capped with an azobenzene. The effect of the isomerization on the unfolding pathway, the force−extension isotherms, and the molecular potential of mean force along the extension coordinate were analyzed using atomistic molecular dynamic simulations and free energy reconstruction techniques.

The unfolding of the trans conformation is characterized by a stable folded phase in which the inner base pair is always intact, an unfolding region in which hydrogen bonds and the stacking interactions between the azobenzene and neighboring bases are broken, and a mechanically stable unfolded conformation. In turn, the unfolding pathway of the cis conformation consists of a globular contracted region with no intact base pairs, a narrow shallow-welled native state with two fully intact base pairs, followed by the unfolded conformation.

These photoinduced changes in the unfolding pathway lead to two possible modes of work extraction through optomechanical cycles.

dx.doi.org/10.1021/ja109071a |J. Am. Chem. Soc. 2011, 133, 3452–3459

In Mode I, the extractable work is due to the disruption of the hairpin structure upon photoisomerization. In turn, Mode II exploits the fact that the trans to cis isomerization effectively reduces the net molecular length. This latter mode is reminiscent of the one used in the experiment by Hugel et al.,[12] while Mode I is unique to the DNA design. These two modes operate in opposite ways, for in Mode I the trans conformation is the stiff version of the molecule while in II the cis conformation is the stiffer structure.

Estimates of the net extractable work during the optomechanical cycle when the pulling is performed with different cantilever stiffnesses indicate that the maximum is obtained when stiff cantilevers are employed. In Mode I the extractable work is 3.4 kcal mol^{-1} with a possible maximum efficiency of 2.4%. Estimates that take into account the quantum yield of the photoisomerization indicate that the efficiency of the process is ~0.4%. This efficiency is five times larger than the one observed in the operation of the poly(azopeptide) optomechanical motor,[13] indicating that the DNA hairpin structure amplifies the transduction effects onset by photoisomerization.

Three major energetic differences between the cis and the trans structures lead to net Mode I work extraction. These are the inner base pair hydrogen bonding energy, the azobenzene-cytosine stacking energy, and the terminal guanine-inner cytosine interaction energy. Terminal base pair hydrogen bonding and normal DNA base stacking are found to be insignificant for work extraction.

These structure−function insights provide the basis for DNA-based motor design. Future prospects include identifying azobenzene-capped structures in which the two modes of work extraction cooperate, studying the effect of temperature, and increasing the hairpin length on the extractable work.

■ ASSOCIATED CONTENT

Supporting Information. Detailed structure of the azobenzene cap and the derived charges; ground state geometries and energies for the cis and trans azobenzene determined using B3LYP/6-31+G**; full citation for ref 38. This material is available free of charge via the Internet at http://pubs.acs.org.

■ AUTHOR INFORMATION

Corresponding Author
schatz@chem.northwestern.edu

■ ACKNOWLEDGMENT

This work was supported by the Nonequilibrium Energy Research Center (NERC) which is an Energy Frontier Research Center funded by the U.S. Department of Energy, Office of Science, Office of Basic Energy Sciences under Award Number DE-SC0000989. MM was supported by the Network for Computational Nanotechnology.

■ REFERENCES

(1) Ritort, F. *J. Phys.: Condens. Matter* **2006**, *18*, R531–R583.
(2) Evans, E. *Annu. Rev. Biophys. Biomol. Struct.* **2001**, *30*, 105–128.
(3) Chen, F.; Tao, N. J. *Acc. Chem. Res.* **2009**, *42*, 429–438.
(4) Rief, M.; Oesterhelt, F.; Heymann, B.; Gaub, H. E. *Science* **1997**, *275*, 1295–1297.
(5) Liphardt, J.; Onoa, B.; Smith, S. B.; Tinoco, I.; Bustamante, C. *Science* **2001**, *292*, 733–737.
(6) Oberhauser, A. F.; Hansma, P. K.; Carrion-Vazquez, M.; Fernandez, J. M. *Proc. Natl. Acad. Sci. U.S.A.* **2001**, *98*, 468–472.
(7) Jarzynski, C. *Eur. Phys. J. B* **2008**, *64*, 331–340.
(8) Park, S.; Schulten, K. *J. Chem. Phys.* **2004**, *120*, 5946–5961.
(9) Hummer, G.; Szabo, A. *Acc. Chem. Res.* **2005**, *38*, 504–513.
(10) Franco, I.; Schatz, G. C.; Ratner, M. A. *J. Chem. Phys.* **2009**, *131*, 124902.
(11) Balzani, V.; Credi, A.; Venturi, M. *Molecular Devices and Machines-Concepts and Perspectives for the Nanoworld*; Wiley-VCH: New York, 2008.
(12) Hugel, T.; Holland, N. B.; Cattani, A.; Moroder, L.; Seitz, M.; Gaub, H. E. *Science* **2002**, *296*, 1103–1106.
(13) Holland, N. B.; Hugel, T.; Neuert, G.; Cattani-Scholz, A.; Renner, C.; Oesterhelt, D.; Moroder, L.; Seitz, M.; Gaub, H. E. *Macromolecules* **2003**, *36*, 2015–2023.
(14) Kumar, G. S.; Neckers, D. C. *Chem. Rev.* **1989**, *89*, 1915–1925.
(15) Griffith, J. *Chem. Soc. Rev.* **1972**, *1*, 481–493.
(16) Bortolus, P.; Monti, S. *J. Phys. Chem.* **1979**, *83*, 648–652.
(17) Dou, Y.; Hu, Y.; Yuan, S.; Wu, W.; Tang, H. *Mol. Phys.* **2009**, *107*, 181–190.
(18) Schaefer, L. V.; Mueller, M.; Gaub, H. E.; Grubmueller, H. *Angew. Chem., Int. Ed.* **2007**, *46*, 2232–2237.
(19) Shi, W.; Giannotti, M. I.; Zhang, X.; Hempenius, M. A.; Schönherr, H.; Vancso, G. J. *Angew. Chem.* **2007**, *46*, 8400–8404.
(20) Lehn, J. M. *Supramolecular Chemistry: Concepts and Perspectives*; Wiley-VCH: New York, 1995.
(21) Collin, J.-P.; Gavina, P.; Heitz, V.; Sauvage, J.-P. *Eur. J. Inorg. Chem.* **1998**, 1–14.
(22) Balzani, B. L.; Credi, A.; Raymo, F. M.; Stoddart, J. F. *Angew. Chem., Int. Ed.* **2000**, *39*, 3349.
(23) Feringa, B. L.; van Delden, R. A.; Koumura, N.; Geertsema, E. M. *Chem. Rev.* **2000**, *100*, 1789.
(24) Yang, Q.-Z.; Huang, Z.; Kucharski, T. J.; Khvostichenko, D.; Chen, J.; Boulatov, R. *Nat. Nanotechnol.* **2009**, *4*, 302–306.
(25) Creatini, L.; Cusati, T.; Granucci, G.; Persico, M. *Chem. Phys.* **2008**, *347*, 492–502.
(26) Neuert, G.; Hugel, T.; Netz, R. R.; Gaub, H. E. *Macromolecules* **2006**, *39*, 789–797.
(27) Asanuma, H.; Liang, X.; Yoshida, T.; Komiyama, M. *Chem. Biol. Chem.* **2001**, *2*, 39.
(28) Liang, X.; Asanuma, H.; Kashida, H.; Takasu, A.; Sakamoto, T.; Kawai, G.; Komiyama, M. *J. Am. Chem. Soc.* **2003**, *125*, 16408.
(29) Liu, M.; Asanuma, H.; Komiyama, M. *J. Am. Chem. Soc.* **2006**, *128*, 1009.
(30) Kang, H.; Liu, H.; Phillips, J. A.; Cao, Z.; Kim, Y.; Chen, Y.; Yang, Z.; Li, J.; Tan, W. *Nano Lett.* **2009**, *9*, 2690–2696.
(31) Tuma, J.; Tonzani, S.; Schatz, G. C.; Karaba, A. H.; Lewis, F. D. *J. Phys. Chem. B* **2007**, *111*, 13101–13106.
(32) Ferrenberg, A. M.; Swendsen, R. H. *Phys. Rev. Lett.* **1989**, *63*, 1195–1198.
(33) Kumar, S.; Bouzida, D.; Swendsen, R. H.; Kollman, P. A.; Rosenberg, J. M. *J. Comput. Chem.* **1992**, *13*, 1011–1021.
(34) Sarzynska, J.; Nilsson, L.; Kulinski, T. *Biophys. J.* **2003**, *85*, 3445–3459.
(35) Sorin, E. J.; Rhee, Y. M.; Pande, V. S. *Biophys. J.* **2005**, *88*, 2516–2524.
(36) Deng, N.-J.; Cieplak, P. *Biophys. J.* **2010**, *98*, 627–636.
(37) Santosh, M.; Maiti, P. K. *J. Phys.: Condens. Matter* **2009**, *21*, 034113.
(38) Case, D. A. et al. *AMBER 10*; University of California: San Francisco, 2008.
(39) Foloppe, N.; MacKerell, A. D. *J. Comput. Chem.* **2000**, *21*, 86–104.
(40) MacKerell, A. D.; Banavali, N. K. *J. Comput. Chem.* **2000**, *21*, 105–120.
(41) Bayly, C. I.; Cieplak, P.; Cornell, W. D.; Kollman, P. A. *J. Phys. Chem.* **1993**, *97*, 10269–10280.
(42) Brown, C. J. *Acta Crystallogr.* **1966**, *21*, 146.

(43) Mostad, A.; Romming, C. *Acta Chem. Scand.* **1971**, *25*, 3561–3568.
(44) Levine, B. G.; Martínez, T. J. *Annu. Rev. Phys. Chem.* **2007**, *58*, 613–634.
(45) Marsili, S.; Procacci, P. *J. Phys. Chem. B* **2010**, *114*, 2509−2516, PMID: 20121079.
(46) Kale, L.; Skeel, R.; Bhandarkar, M.; Brunner, R.; Gursoy, A.; Krawetz, N.; Phillips, J.; Shinozaki, A.; Varadarajan, K.; Schulten, K. *J. Comput. Phys.* **1999**, *151*, 283–312.
(47) McCullagh, M.; Zhang, L.; Karaba, A. H.; Zhu, H.; Schatz, G. C.; Lewis, F. D. *J. Phys. Chem. B* **2008**, *112*, 11415–11421.
(48) Pohorille, A.; Ross, W. S.; Tinoco, J. I. *Int. J. Supercomput. Appl.* **1990**, *4*, 81–96.
(49) Krautbauer, R.; Rief, M.; Gaub, H. E. *Nano Lett.* **2003**, *3*, 493–496.
(50) Hagan, M. F.; Dinner, A. R.; Chandler, D.; Chakraborty, A. K. *Proc. Natl. Acad. Sci.* **2003**, *100*, 13922–13927.